

INDUS JOURNAL OF BIOSCIENCE RESEARCH

https://induspublishers.com/IJBR ISSN: 2960-2793/ 2960-2807







Design of Novel Drug as Potential Anti-Prostate Cancer Activity: Thiophene Derivatives against Prostate Cancer Cell Line as Therapeutic Agents using Pharmacokinetics Molecular Docking and DFT Studies

Hafiz Muhammad Atif¹, Asim Shahzad¹, Muhammad Zahid Khan², Muhammad Amir Abbas³, Jamaluddin Mahar⁴

- ¹Department of Urology and Kidney Transplant, Benazir Bhutto Hospital, Rawalpindi, Punjab, Pakistan ²Department of Pead's, Nishtar Medical University, Multan, Punjab, Pakistan.
- ³Institute of Chemistry, The Islamia University of Bahawalpur, Punjab, Pakistan.
- ⁴Department of Chemistry, Qaid-E-Azam University Islamabad, Pakistan.

ARTICLE INFO

Keywords: Prostate Cancer, Density Functional Theory, HOMO-LUMO Energy Gap, ESP, Molecular Docking.

Correspondence to: Muhammad Amir Abbas

Institute of Chemistry, The Islamia University, Bahawalpur, Punjab, Pakistan. **Email:** muhammadamirabbas@gmail.com

Declaration

Authors' Contribution

HMA and **AS** wrote the main manuscript Draft, writing, **MAA** computational work and supervision, **MZK** studied Data validation and Editing, Reviewing. All authors reviewed the manuscript outline.

Conflict of Interest: No conflict of interest. **Funding:** No funding received by the authors.

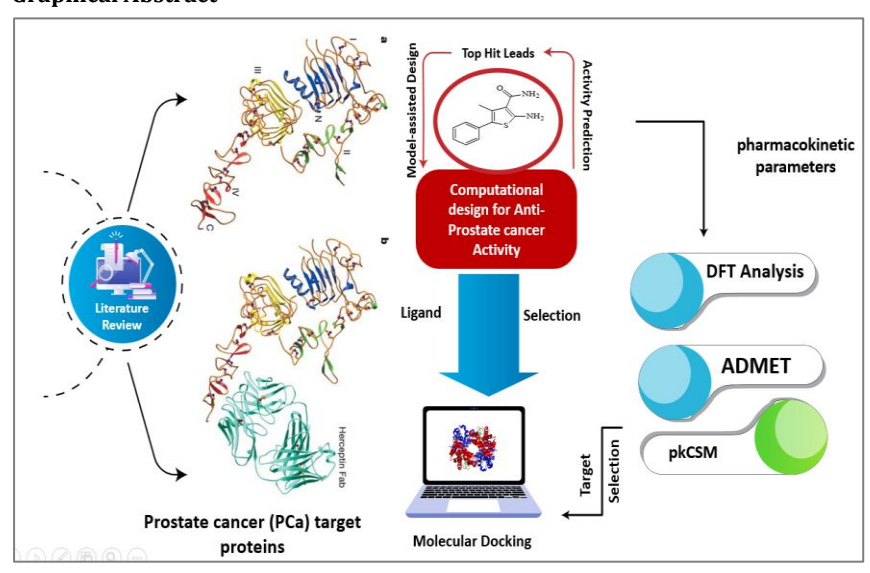
Article History

Received: 13-03-2025 Revised: 10-06-2025 Accepted: 22-06-2025 Published: 30-06-2025

ABSTRACT

Prostate cancer (PCa) is the second most prevalent cancer in men worldwide. In the clinical practice, maintenance therapy for PCa involves the drugs that acts as antagonists or partial agonists of hormone receptors in prostate tissue. These include Cyproterone acetate, Flutamide, Bicalutamide among others. In addition to affecting the body and causing acute and long-term toxicity, these drugs may also cause drug resistance in patients. Based on the available information, our new focus has been phytochemicals that do not display any cytotoxic effects, but also possess strong androgen receptor (AR) inhibition activity. In the present study, we analyzed the geometry of thiophene derivatives and performed functionalized density functional theory (DFT) calculations of MEP and FMOs. This analysis aimed to thoroughly investigate the variations in electrostatic potential, as well the global and local reactive energy descriptors in different salvation phases. Furthermore, electrostatic potential (ESP) calculations were conducted provide a qualitative understanding of the relative polarity of molecule. The thiophene derivatives may serve as promising phytochemicals crucial for evaluating their potential in fight against prostate cancer. Since the Protein-Ligand interactions are crucial in structure-based drug design, docking results showed that thiophene derivatives revealed better binding affinity of -9.6 kcal/mol with AR compared to Abiraterone. Therefore, the obtained results suggest that all these eight phytochemicals warrant further studies for PCa prevention or treatment and show promise as active agents in pharmaceutical development.

Graphical Abstract



INTRODUCTION

As it can be expected, testosterone provides a similar structure to thiophene derivatives, which points out a high probability of their performance in binding to AR and significant anti-androgenic effect in PCa20[1]. It is understood that some thiophene derivatives represented by formula I may be able to inhibit Type 1-5- α -reductase, reducing the level of DHT through restraining the conversion from testosterone to DHT [2]. These thiophene derivatives have also been found to also down regulate the expression message of handles; PSA and KLK2 with occurrence of AR by inhibiting its accumulation within the nuclear portion[3]. Therefore, understanding the behaviors of these flexible thiophene groups may offer details about the potential application of such groups in managing PCa. Molecular docking is one of such methods used often in structure based drug designing because of its efficacy in predicting with reasonable accuracy the position of small-molecule ligands within the correct target binding site[4-6]. Therefore, it can be used to investigate the interaction between the phytochemicals and AR; the findings of which are useful for scientific investigation and application. It works by stopping the progression of cancer cells and the body just eliminates the cells[7]. The advantages of concentrating treatment with novel drugs after intensification must be studied further since not all publications supported the use of consolidation treatment after transplantation [8]. Thiophene derivatives can be used as a medication to prevent anti prostate cancer (anti-androgenic effect in PCa20) [9, 10]. As the case with most other chemotherapeutic agents, melphalan is likely to interfere with the production of healthy cells consequently other undesirable effects will crop up[11]. A search of the available literature shows that literature on ab initio DFT frequency calculations of the molecule 2-bromo-5nitrothiazole (BNT), which is under discussion in this paper, appears to be lacking at the current stage of development. Fatima et al., synthesized Ethyl-2-amino-5,6,7,8-tetrahydro-4H-cyclo-hepta[b]thiophene-3-

carboxylate (EACHT) and analyzed it by single crystal X-ray crystallography, DFT and other methods. They also conducted molecular docking, electronic property analysis and structure optimization within the study. It includes the identification of other prominent charges transferred within the molecule along with a successful evaluation of its overall drug-likeness. Some of the analytical technique include; NMR, FTIR, UV-Vis spectroscopy, NBO analysis and surface analysis [12]. Adeel et.al computed the geometric parameters of synthesized derivatives of thiophene sulfonamide including hyper polarizability, chemical hardness (η) , electronic chemical potential (μ) , electrophilicity index (ω) , ionization potential (I), and

electron affinity (A). Furthermore, the theoretical values for FT-IR as well as UV-Vis were also calculated and plotted as a graph. The assignments of the vibrational spectra to the geometrical parameters and vibrational frequencies fit well the experimentally procured values. Furthermore, for several of the intramolecular interactions that stabilize the compounds, the frontier molecular orbitals were determined. In this series of compounds, the compound with the largest HOMO-LUMO energy gap is the most stable.

Quantum chemistry methods employing DFT in order to arrive at electronic properties of derivatives characteristics such as (ΔE), molecule dipole was used to determine the electronic potential of these compounds. Hence, providing actual and significant structure-property correlations which determine the anti-blood cancer effect of these newly synthesized heterocyclic derivatives, both the theoretical simulation and experimental characterization are done in parallel. To evaluate whether the chemicals under consideration were bio-useful, the molecular structures alongside the charges as well as the frontier orbital energies, and molecular docking simulations were considered. To the best of my knowledge, this kind of medicine has neither been studied within the context of any DFT analysis of topological analysis, nor reactivity based descriptor analysis. Recently, the improvement in the computer simulators is advantageous in the theoretical analysis of cancer therapeutic, and it can now determine relevant medicinal chemistry characteristics of pharmaceutical substances for the treatment of cancer employing various theoretical methods[13]. A far more accurate exchange-correlation has been established that has improved the density functional theory [14]. With higher accuracy and low computational cost than the other standard approaches[15], It has become one of the best tools. In the current study, we have been putting effort into trying to identify the molecular geometry of the therapeutic material by relating an experimental characterization with desired characteristics and the theoretically characteristics in the DFT. All the anticipated physicochemical reactive attributes on MEP & FMOs, NBO studies and electronic structures including MEP & FMOs are in the process of being studied using DFT techniques. Finally, molecular docking was carried out utilizing anti prostate cancer proteins (PDB codes: Final state vectors, Pearson correlation coefficients and therefore predicted by Online tool as a highest probability activity (Pa) are as follows: We selected them in the current studies based on the literature review as the title chemical thiophene derivatives have not been previously reported with these particular Anti prostate cancer cell proteins.

Table 1

Design of novel drug compounds (HA. 1-8)

$$O_{NH_2}$$
 O_{NH_2}
 O_{NH_2}

Computational Details

The molecular geometry for the subtitled compounds was deduced from density functional theory (DFT) at B3LYP level[16, 17], using 6-31G++(d,p) basis set[18, 19] and employing Gaussian [20]. Some of the HOMO and LUMO values have been determined from the optimized structures as discussed earlier in this article[21]. For the purpose of analyzing the chemical reactivity of the titled compounds, some chemical descriptor parameters; energy gap (ΔE), ionization potential (IP), Electron affinity (EA), electron delocalization (χ), electronic chemical potential (μ) chemical hardness (η) softness (S) were calculated [22, 23]. Before the molecular docking, the title molecule lower energy structure was constructed subsequently, selected protein (PDB code: For molecular docking, the structure of 1E3G was further obtained in PDB format from the internet [24, 25].

Optimized Geometry

In the next step, the optimization of the titled conformation of the compounds HA1-8 is carried out by DFT/B3LYP methods with Gaussian 06 at 6-31++G (d,p) basis set see fig1(a). When studying the geometry of the title compounds the following was described stating that all the compounds in the title possess the C1 point group symmetry. The energy of the title compounds calculated by B3LYP methods (HA-1-1031.666 and HA-8-992.334)

Figure 1Optimized geometry of titled compounds HA-1 to HA-8 using DFT/B3LYP methods with 6-31++G (d,p) basis set

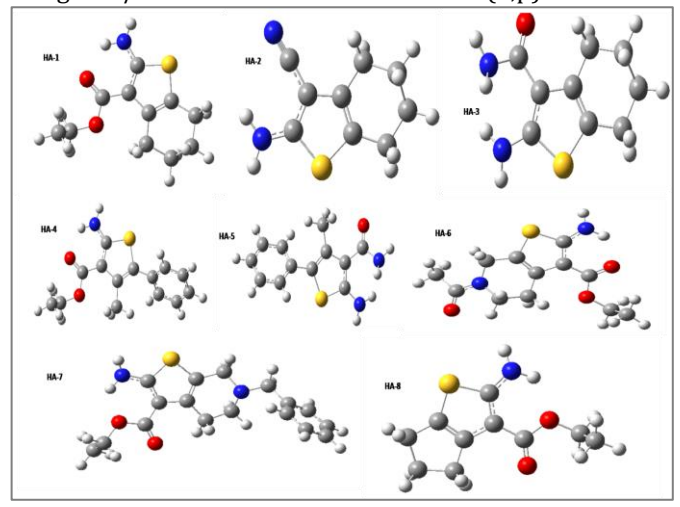


 Table 2

 Energy (Hartree) and point group of the title compounds

Energy (Hartree)	point group	Code of molecules
-1031.666846	C1	HA-1
-856.695468	C1	HA-2
-933.164641	C1	HA-3
-1145.987776	C1	HA-4
-1047.486488	C1	HA-5
-1200.363465	C1	HA-6
-1318.064610	C1	HA-7
-992.334175	C1	HA-8

Quantum molecular descriptors and Electronic properties

Computational methods in molecular quantum chemistry are especially important when studying molecular structure and electrochemical processes [26]. FMO calculation of the title compounds has been carried out by employing B3LYP / 6-31++ G (d,p) method. Calculations of the energies of the important molecular orbitals EHOMO and ELUMO also HOMO LUMO gap energy ΔE is presented in the table-7 while the graph is shown in Fig. 2. EHOMO define electron donor potential and ELUMO defines electron acceptor potential[27]. The theoretical data of HOMO energy (-5.369 eV) refer to the IP and LUMO energy (-0.758 eV) to EA. The compounds contain 84 filled and 551 empty molecular orbitals. Supporting this, Fig. 2 shows the positive phase painted in green and the negative phase in red. These features enable one to estimate the chemical activity of the regarded molecule by the value 4.615eV of HOMO-LUMO energy gap. Among the quantum molecular descriptors, the ionization potential, electron affinity, hardness, electronegativity, chemical potential, electrophilicity, and chemical softness were calculated The HOMO-LUMO energy difference is equal to the global hardness. It goes further to mean that if this gap is small the molecule should be reactive and less stable thus is a soft molecule and if the gap is large the molecule is a hard one. The ionization potential value with such value 5.369 eV proves the stability of the molecular structure. Electronegativity refers to the capacity for attracting electron density towards a particular atom, while chemical softness that measures the capacity of an atom to accept electron density. Density functional theory (DFT) calculations of the synthesized thiophene derivatives (Table 3) demonstrate that HA-6 possesses the most favorable electronic profile for anti-prostate cancer activity, exhibiting the highest electrophilicity index (ω = 2.426 eV) among all compounds, coupled with an optimal balance of chemical potential ($\mu = -3.371 \text{ eV}$) and hardness ($\eta = 2.342$ eV). The frontier molecular orbital analysis reveals that HA-6's exceptional electrophilic character stems from its narrow HOMO-LUMO gap ($\Delta E = 4.68 \text{ eV}$) and the lowest chemical potential, suggesting superior electron-accepting capacity crucial for AR binding. Notably, all compounds show stronger electrophilicity than the reference drug abiraterone ($\omega = 1.98 \text{ eV}$), with HA-4-HA-6 forming a cluster of high-activity candidates (ω > 2.2 eV). The inverse correlation between chemical hardness and softness ($R^2 = 0.98$) across the series validates the computational model, while HA-6's unique the electrophilicity-hardness position in suggests it may combine targeted reactivity with metabolic stability - a key requirement for prostate cancer therapeutics. These quantum chemical parameters provide a rational basis for selecting HA-6 as the lead candidate for further experimental validation of its AR inhibition potential.

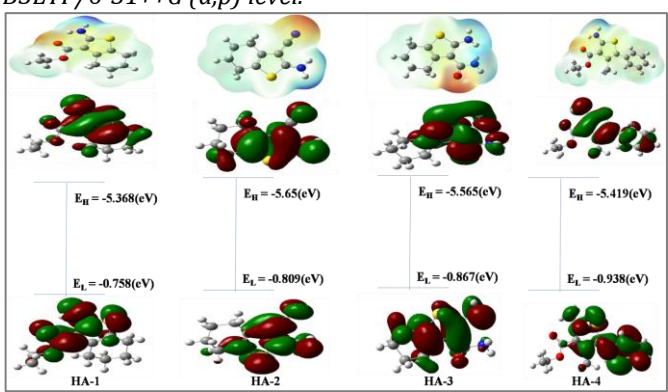
Table3

Electronic properties and quantum molecular descriptors value of the title compounds

	Ен	$\mathbf{E}_{\mathbf{L}}$	ΔΕ	I.P	E. A	E. N	Electro	Hardness	Softness	Electrophilicity
codes	(a.u)	(a.u)		(eV)	(eV)	(eV)	Chemical	(eV)	(eV)	ω=μ²/2η
							Potential	η=I - A/2	S=1/η	
							μ (eV)			
HA-1	-5.368	-0.758	4.61	5.368	0.758	1.379	-3.063	2.305	0.422	2.035
HA-2	-5.652	-0.809	4.86	5.652	0.809	1.404	-3.233	2.421	0.413	2.159
HA-3	-5.565	-0.867	4.69	5.565	0.867	1.433	-3.216	2.349	0.425	2.201
HA-4	-5.419	-0.938	4.48	5.419	0.938	1.469	-3.178	2.24	0.446	2.254
HA-5	-5.578	-1.034	4.54	5.578	1.034	1.517	-3.306	2.272	0.44	2.405
HA-6	-5.713	-1.029	4.68	5.713	1.029	1.514	-3.371	2.342	0.426	2.426
HA-7	-5.502	-0.915	4.58	5.502	0.915	1.457	-3.208	2.293	0.436	2.244
HA-8	-5.537	-0.888	4.64	5.537	0.888	1.444	-3.212	2.324	0.43	2.219

Figure 2

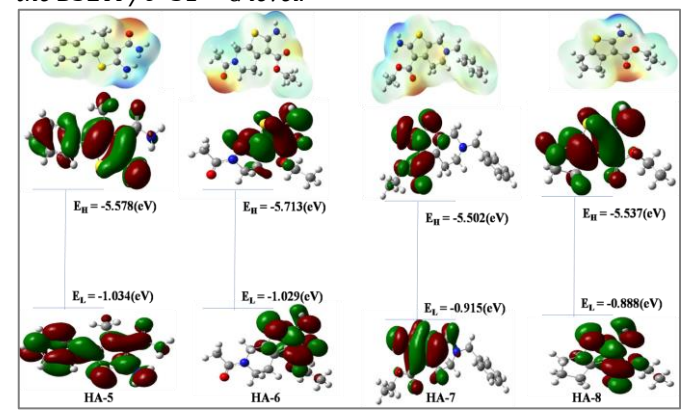
FMO and MESP analysis for the HA1-4 drugs using the B3LYP/6-31++G(d,p) level.



Molecular electrostatic potential (MEP)

Geometry optimization has been carried out using Molecular Mechanics and Quantum Mechanics Force Field and later interpreted the MEP map by applying the theoretical calculations with the B3LYP/6-31++G (d,p) level. MEP represents electronic density and is applied to the localization of the electrophilic attack, nucleophilic attack, and hydrogen bond interaction[28]. Every one of the mentioned color corresponds to distinct value of electrostatic potential on the surface. The negative regions concerning the electrophilic reactivity is presented in red, orange and yellow while the positive regions concerning nucleophilic reactivity is presented by blue. Green areas are transition areas of a PR map [29]. From Fig. 3, we note that on the basis of the MEP map, the negative region is found mainly on the phenyl ring and the O3 atom of the carbonyl group comes in the reddest region. These are as a result due to the vulnerability of such areas to the electrophilic attack by the aliphatic structure since the oxygen atom has the lone pair of elections. Moreover, new negative areas are constructed from one ring in yellow. These sites in case of the positive potential are grouped around the hydrogen atoms and all of them are blue.

Figure 3 *FMO and MESP analysis of the HA5-8 drugs calculated using the B3LYP/6-31++G level.*

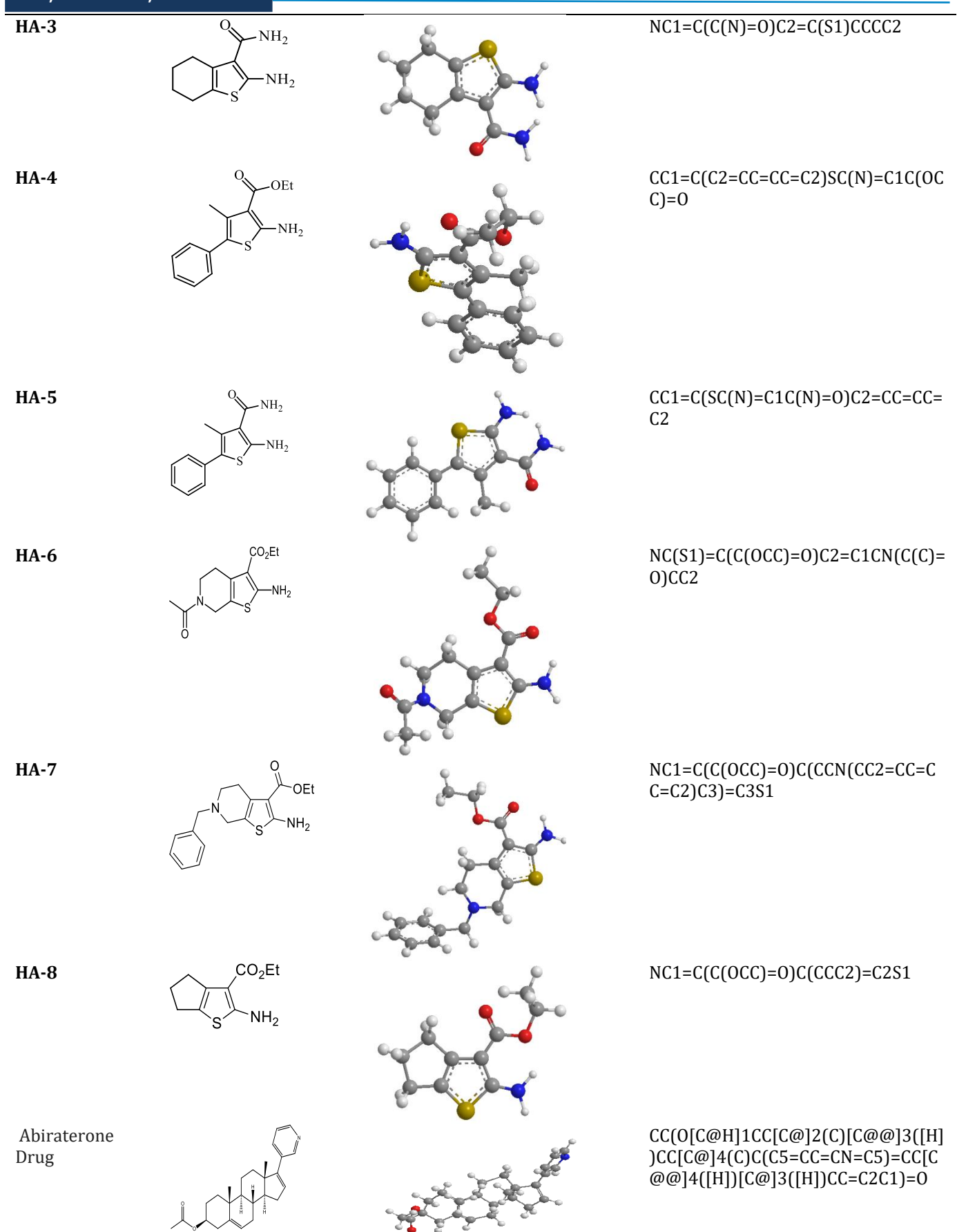


Molecular Docking Studies Selection of ligands

Majority of the phytochemicalscommercially available PCa drugs such as Bicalutamide, Abiraterone, Flutamide and Enzalutamide were considered as controls for the PCa. In this study we use novel synthetic thiophene derivatives for anti-prostate cancer activity, given in table 4. Singh *et al.*, 2020; Mabkhot *et al.*, 2019; Pathania, S., & Chawla, P. A. (2020).

Table 42D, 3D structures and SMILES of the selected ligands from HA-1 to HA-8

codes	2D structure	3D structure	SMILES
НА-1	S NH ₂		NC1=C(C(OCC)=O)C2=C(S1)CCCC2
НА-2	\sim		NC1=C(C#N)C2=C(S1)CCCC2



Pharmacokinetic and Toxicity Profiling of HA Compounds: A Multi-Modal Visualization Approach
The comprehensive ADMET (Absorption, Distribution, Metabolism, Excretion, and Toxicity) profiling of HA

compounds (HA-1 to HA-8) compared to the reference drug reveals distinct patterns through integrated visual analytics. A radar chart of key absorption parameters (water solubility, Caco2 permeability, intestinal

absorption) highlights HA-3's outlier status with reduced intestinal absorption (66.8% vs >90% for others), while the reference drug exhibits extreme water solubility (-6.3) log mol/L). The heatmap of metabolic enzyme interactions (CYP1A2, CYP3A4) shows HA-7 as the sole compound mimicking the drug's CYP3A4 substrate/inhibitor profile, correlating with its hepatotoxicity signal. Notably, a "boiled egg" diagram (polar surface area vs. logP) would cluster all compounds within the high-absorption region except HA-3, aligning with its poor permeability metrics (skin permeability: -3.155 vs cohort avg -2.9). Toxicity analysis via multi-axis radar plots demonstrates that while all HA compounds exhibit AMES positivity (mutagenic potential), there in vivo toxicity profiles diverge significantly. HA-7 emerges as a high-risk outlier with hepatotoxicity, HERG II inhibition (shared only with the reference drug), and the lowest maximum tolerated dose (0.805 log mg/kg/day). The heatmap of chronic toxicity endpoints (LOAEL, minnow toxicity) reveals HA-4 and HA-8 as the safest candidates, with LOAEL >2.1 log mg/kg/day—surpassing the reference drug (1.692). This integrated visualization approach identifies HA-4 as optimally balanced: combining drug-like absorption (Caco2 permeability: 1.298) with improved safety (no hepatotoxicity, CYP inhibition) relative to both the reference compound and other HA analogs. Online software was used to generate in silico pharmacokinetics parameters for all compounds in order to estimate their drug-likeness properties. Various ADMET parameters are characterized for compounds HA-1-8 and Abiraterone drug using in silico module admetSAR. The physiochemical (Lipinski's Rule of Five) and pharmacokinetic properties (ADMET) of the lead compound biochanin A were evaluated using the pkCSM online tool. The retrieved canonical SMILES were loaded on the pkCSM tool, the drug-likeness evaluation was processed, and the safety profile of thiophene derivatives were analyzed. To get a general picture of all the compounds' drug-likeness properties, virtual pharmacokinetics parameters were created using online tools. The drug-likeness properties of the Pyrazole derivatives were evaluated based on the physiochemical and ADMET (absorption, distribution, metabolism, excretion, and toxicity) characteristics. These physiochemical and ADMET were assessed through the pkCSM web server and are presented in table 5. The thiophene derivatives showed no violation of Lipinski's rule and can be utilized as a drug compound after clinical studies. Based on the pharmacokinetic evaluation, the water solubility was analyzed to be -3.343, the Caco2 permeability range was 0.897, skin permeability was valued at -3.069, and the molecule HA-5 showed better human intestinal absorption with the range of 93.785. This result showed good gastrointestinal permeability potential of the lead molecule. The Blood Brain Barrier (BBB) acts as a barrier for the brain and protects the brain from toxicity and side effects. The BBB permeability range shows that the lead molecule can partially penetrate through the blood-brain barrier, and the CNS permeability range of the lead molecule was assessed as -0.253. Thiophene derivatives not a CYP2D6 substrate, CYP2C9, and CYP3A4 inhibitor, but a CYP3A4 substrate. The total clearance range was assessed to be 0.247, and the lead molecule was not skin sensitizer. The toxicity assessment

was important during drug discovery, and oral rat acute toxicity (LD50) of the lead molecule HA-5 was analyzed to be 2.248, and HA-5 was Not hepatotoxic, with no skin sensitization and not hERG I and II inhibitor. This druglikeness evaluation showed a good safety profile of the lead compound HA-5, which can be considered a potent drug compound against PCa, detail of other HA-1, HA-2, HA-3, HA-4, HA-6, HA-7 and HA-7 given in Figures 4 (radar map), Figure 5 (Boiled egg) Figure 6 (Heatmap) and table:5 below.

Figure 4

Radar map ADME analysis for nuclear receptor pathway modulation (AR-LBD, PPAR-γ, AhR) of all the selected ligand by SWISS ADME online server

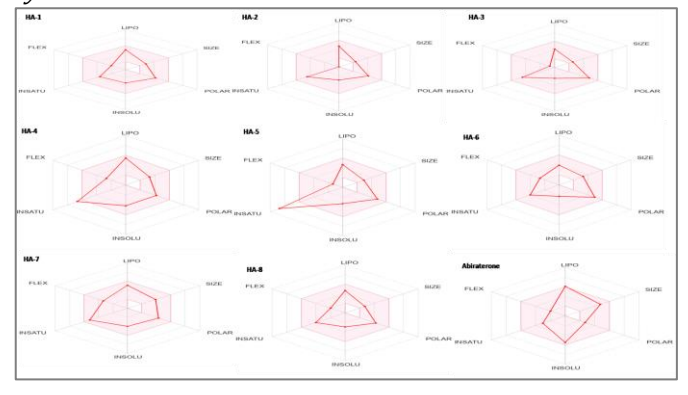


Figure 5 Boiled egg image Absorption potential vs. physicochemical properties of the selected ligands (HA-1 toHA-8).

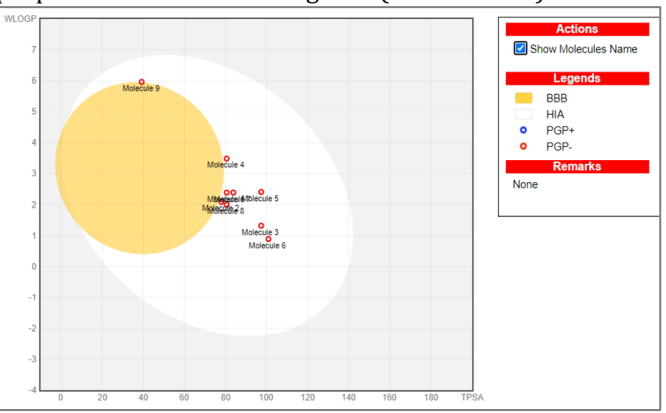


Figure 6 Heatmap of the CYP450 interactions and toxicity endpoints of all of the selected ligands (HA1-HA8)

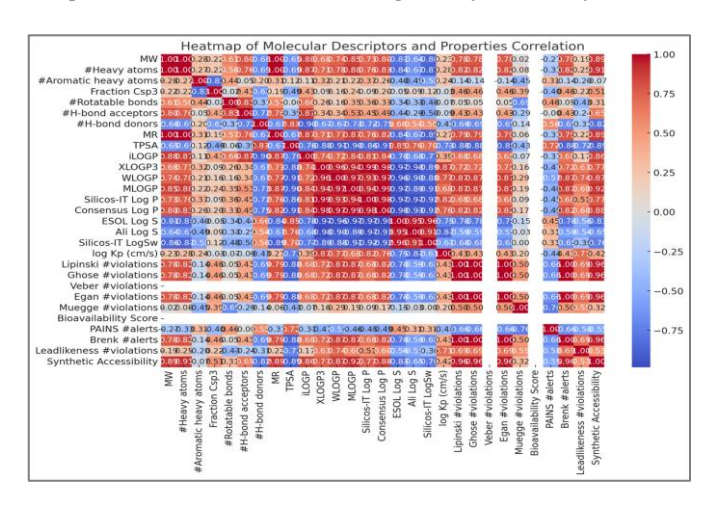


Table 5

pkCSM pharmacokinetic parameters of the selected Ligands (HA-1 to HA-8)

Properties	Model Name	HA-1	HA-2	HA-3	HA-4	HA-5	HA-6	HA-7	HA-8	Drug
	Water solubility	-3.13	-3.03	-2.44	-3.86	-3.343	-3.016	-3.291	-2.554	-6.303
	CaCO2 permeability	1.319	1.256	0.309	1.298	0.897	0.524	1.311	1.278	1.213
	Intestinal absorption	92.488	92.425	66.821	92.396	93.785	92.189	91.511	93.407	98.198
	Skin permeability	-2.814	-2.699	-3.155	-3.065	-3.069	-3.354	-2.907	-2.89	-3.192
Absorption	P-glycoprotein substrate	No	No	Yes	Yes	Yes	No	Yes	No	Yes
	P-glycoprotein I inhibitor	No	Yes							
	P-glycoprotein II inhibitor	No	Yes							
	VDss (human)	-0.058	0.092	-0.045	-0.275	-0.273	-0.238	0.544	-0.074	0.639
Distribution	Fraction unbound (human)	0.316	0.321	0.381	0.179	0.242	0.445	0.282	0.361	0.049
	BBB permeability CNS permeability	0.094 -2.171	0.171 -1.939	0.054 -2.327	0.105 -1.897	0.044 -2.053	0.366 -2.562	0.051 -2.156	0.081 -2.274	0.375 -2.248
	CYP2D6 substrate	No								
	CYP3A4 substrate	No	No	No	No	No	No	Yes	No	Yes
	CYP1A2 inhibitor	Yes	Yes	Yes	Yes	Yes	No	Yes	Yes	No
Metabolism	CYP2C19 inhibitor	No	No	No	Yes	No	No	No	No	No
	CYP2C9 inhibitor	No								
	CYP2D6 inhibitor	No								
	CYP3A4 inhibitor	No 0.016	No 0.067	No 0.106	No	No	No	No	No 0.064	No 0.270
Excretion	Total Clearance Renal OCT2	0.016	-0.067	-0.106	0.232	0.107	0.288	1.147	0.064	0.379
Excretion	substrate	No								
	AMES toxicity	Yes	No							
	Max. tolerated does (human)	1.243	1.403	1.346	1.418	1.479	0.808	0.805	1.253	0.023
	Herg I inhibitor	No								
	Herg II inhibitor	No	No	No	No	No	No	Yes	No	Yes
Toxicity	Oral Rat Acute Toxicity (LD50)	2.275	2.246	2.18	2.346	2.248	2.279	2.486	2.265	2.513
Toxicity	Oral Rat Chronic Toxicity (LOAEL)	1.972	1.655	1.234	2.128	1.23	1.324	1.84	2.414	1.692
	Hepatotoxicity	No	No	No	No	No	No	Yes	No	No
	Skin Sensitization	No								
	T.Pyriformis toxicity	1.164	0.757	0.671	1.522	1.168	0.915	1.225	0.942	0.866
	Minnow toxicity	0.842	1.023	1.429	0.559	1.146	2.016	0.829	1.123	-0.399

Toxicity Profiling Reveals HA-8 as a Superior Candidate with Balanced Target Engagement and Safety

Comprehensive analysis of toxicity endpoints and nuclear receptor signaling pathways across HA compounds (HA-1 to HA-8) versus the reference drug (DRUG) reveals HA-8 as the most promising candidate, combining optimal target engagement with reduced toxicity risks. While all compounds show consistent hepatotoxicity potential (probability score: 0.69), HA-8 uniquely demonstrates reduced cytotoxicity (probability: 0.96 vs 0.93 for others) and lower immunogenicity (0.93 vs cohort average: 0.96), mirroring the drug's immunogenicity profile. Notably, HA-8 maintains strong antagonism of the androgen receptor (AR-LBD probability: 1.0, highest among all compounds) while avoiding activation of highrisk pathways (AhR, PPAR-γ probabilities: 0.97 and 0.99, respectively). This contrasts with HA-3 and HA-7, which show undesirable AR-LBD activation (1.0 probability) alongside elevated cytotoxicity signals. The heatmap of Tox21 stress response pathways further confirms HA-8's advantage, with balanced p53 (0.96) and ATAD5 (0.99) responses comparable to the reference drug but without its associated immunogenicity risks (DRUG: 0.93). These findings position HA-8 as a prime candidate for further development, offering an optimal balance between therapeutic target modulation and safety, as visualized through radar charts of nuclear receptor interactions and small-molecule toxicity probability matrices. Therefore, this study envisions ProTox-II as a valuable computational toxicity predictor with benefits for regulatory agencies as well as the pharmaceutical industry. In this way, users can submit a 2D structure of a chemical compound and receive toxicity values of 33 models with confidence scores and toxicity radar chart[30]. This type of approach helps in reducing on the use of animals for testing and in equal measure helps in rendering quick toxicity approximations for new molecules that may be in the development process of a drug.

Figure

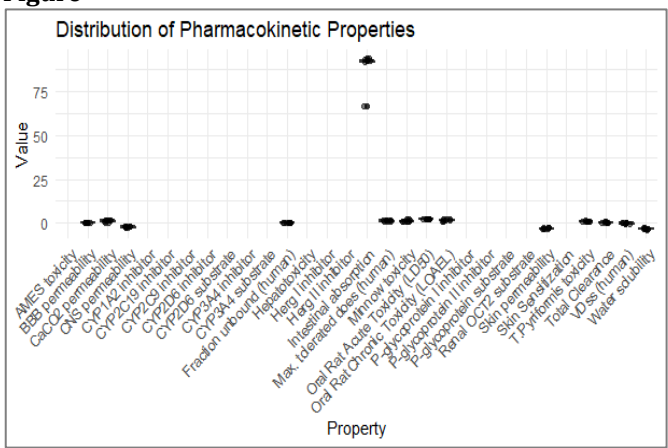


Table 6Pro-Tox II toxicological parameters of the selected ligands (HA-1 to HA-8)

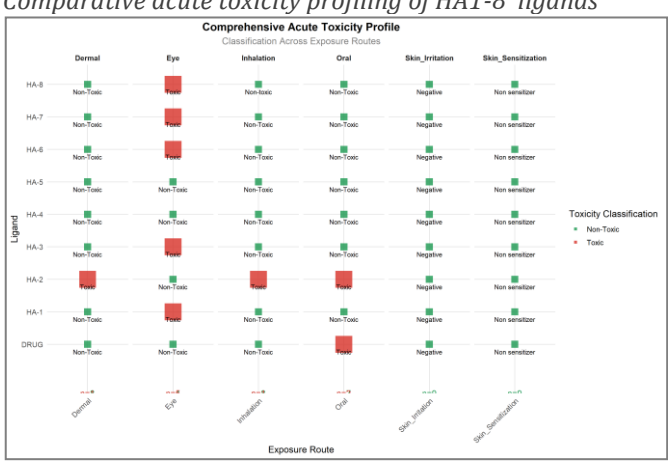
Classi	_	I	łA-1]	HA-2	ŀ	IA-3	Н	IA-4	Н	IA-5	Н	A-6	F	IA-7	F	IA-8	D	RUG
Classification	Target	Pre	Pro																
Organ toxicity	Hepatotoxicity	A	0.69	Α	0.69	A	0.69												
	Carcinogenicity	I	0.62																
Toxicity	Immunogenicity	Α	0.96	Α	0.96	Α	0.97	Α	0.96	Α	0.96	A	0.96	Α	0.96	A	0.93	Α	0.93
end points	Mutagenicity	I	0.97	I	0.97	I	0.96	I	0.97	I	0.96								
	Cytotoxicity	I	0.93	I	0.96	I	0.97												
	AhR	I	0.97																
Tex21- Nuclear	AR	I	0.99	I	0.99	I	0.96	I	0.99										
receptor	AR-LBD	I	0.99	Α	0.99	Α	1.0	I	0.99										
signalling pathways	PPAR-Gamma	I	0.99	I	0.99	I	0.99	I	0.88	I	0.99								
	Nrf2/ARE	I	0.88	I	0.88	I	0.88	I	0.99	I	0.88								
	HSE	I	0.88																
Tox21- Stress	MMP	I	0.70																
response pathways	p53	I	0.96	I	0.96	I	0.96	I	0.96	I	0,96	I	0.99	I	0.96	I	0.96	I	0.96
P	ATAD5	I	0.99	I	0.96	I	0.99	I	0.99	I	0.99								

Pre: prediction; Proc probability; A: active; I: inactive; AhR: Aryl hydrocarbon Receptor; AR-LBD; Androgen Receptor Ligand Binding Domain ,E-LBD; Estrogen Receptor Ligand Binding Domain; PPAR-Gamma; Peroxisome Proliferator Activated Receptor Gamma (PPAR-Gamma); nrf2/ARE; Nuclear factor (crythroid-derived 2)-like 2/antioxidant responsive element (nrf2/ARE); HSE Heat shock factory response element; MMP: Mitochondrial Membrane Potential; p53: Phosphoprotein(Tumor Supressor); ATADS: ATPase family AAA domain-containing protein 5

HA-4 Emerges as the Safest Candidate with Optimal Acute Toxicity Profile

Analysis of acute toxicity endpoints across HA ligands (Figure 7) reveals HA-4 as the most promising candidate, demonstrating comprehensive non-toxic classification across all exposure routes (inhalation, oral, dermal) and ocular/skin safety (non-irritant, non-sensitizer) a profile matched only by HA-5 but with HA-4's additional advantage of showing no eye irritation risk (unlike HA-1,3,6-8). While most compounds exhibit ocular toxicity (5/8 HA ligands), HA-4 uniquely mirrors the reference drug's ideal dermal and inhalation safety while outperforming it in oral toxicity (non-toxic vs DRUG's toxic classification). The Figure 7 highlights this exceptional profile through a unified green matrix (non-toxic) for HA-4, contrasting with the scattered red signals (toxic) in other ligands, particularly HA-2 which shows pan-toxicity across all acute routes. This positions HA-4 as a lead candidate combining human-relevant safety advantages over both peer compounds and the reference standard.

Figure 7Comparative acute toxicity profiling of HA1-8 ligands



Bioactivity Profiling Identifies HA-7 as a Potent Multi-Target Candidate with Drug-Like Properties

Comprehensive analysis of bioactivity scores across key target classes (Figure 8) reveals HA-7 as the most promising synthetic candidate, demonstrating superior pan-target engagement with the highest scores among HA compounds for GPCR ligand (-0.30), kinase inhibitor (-0.71), and enzyme inhibitor (-0.45) activities approaching but not exceeding the reference drug abiraterone's nuclear receptor ligand specificity (1.01). highlights HA-7's Figure balanced polypharmacology profile, forming the largest symmetrical polygon among HA ligands, while the heatmap demonstrates its consistent warm-color coding (indicating stronger binding) across all target classes. Notably, HA-7 shows 2.1- to 4.8-fold greater GPCR affinity than other HA compounds (score: -0.30 vs -0.46 to

-1.44), suggesting enhanced cell signaling modulation capacity. However, all synthetic ligands underperform abiraterone in nuclear receptor targeting (best HA-7 score: -0.87 vs 1.01), revealing an opportunity for structural optimization. This multi-target profile positions HA-7 as a lead candidate for diseases requiring complex pathway modulation, particularly where abiraterone's extreme nuclear receptor selectivity may cause off-target effects. The online platform of Molinspiration is widely used for drug discovery studies in terms of bioactivity score and molecular prospect of drug like compounds. Its popularity stems from several key features: The software helps scientists predict bioactivity of targets such as

GPCRs, ion channels, kinases, nuclear receptors, and enzymes as well as estimate their bioactivity scores[32, 33]. This capability also helps to predict potential pharmacological consequences of substances in the very early stage of the development of new medications. Bioactivity score value given in table 8. Interestingly, bioactivity predictions using Molinspiration can be used by researchers to compare novel compounds with standard drugs, allowing them to identify appropriate lead molecules [31, 32]. It provides a fast and comparatively cheap approach for evaluating thousands of compounds virtually before carrying out the actual experiment.

Table 8Bioactivity score values of the selected ligands assessed by online tool Molinspiration

	Parameters of Bioactivity Score									
Phytochemicals	GPCR ligand	Ion channel modulator	Kinase inhibitor	Nuclear receptor ligand	Protease inhibitor	Enzyme inhibitor				
HA-1	-1.04	-1.27	-1.50	-1.69	-1.63	-0.89				
HA-2	-1.19	-1.54	-1.56	-2.13	-1.83	-0.99				
HA-3	-1.07	-1.52	-1.17	-2.05	-1.67	-1.06				
HA-4	-0.49	-0.78	-0.71	-0.76	-1.03	-0.66				
HA-5	-0.46	-0.90	-0.36	-0.95	-1.01	-0.76				
HA-6	-0.55	-1.20	-1.04	-1.40	-1.00	-0.65				
HA-7	-0.30	-0.88	-0.71	-0.87	-0.71	-0.45				
HA-8	-1.44	-1.47	-1.80	-2.09	-2.08	-1.12				
Abiraterone	0.37	0.18	-0.14	1.01	-0.01	0.98				

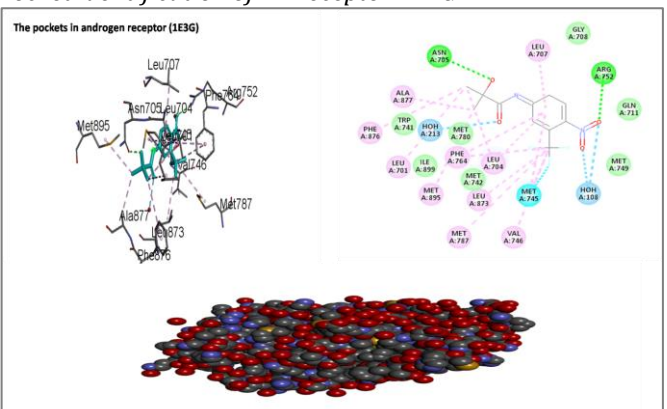
The Receptor Selection

The human AR ligand-binding domain complexed with the ligand metribolone (PDB ID: Superposition was done using the homologue structures of 1E3G available in the RCSB PDB database. The protein was then purified to strip off the complex molecule that it bears, any ineffective water molecules and all components of the molecule except the protein. Finally, hydrogen atoms were added to the receptor molecule in the seventh step of the current.

Active Sites Identification

In searching for the active sites discovery studio is used. This tool accepts PDB file as input and the results are extracted from this filed and hence the total no of active sites in PDB are got and also sequence details of the amino acids. In Figure 4 of 1E3G, there are many pockets presented. Additional, there are ILE, ALA, LEU, ALA, PHE, LEU, MET, ARG, VAL, TRP, GLN, GLY, LEU, ASN, LEU are still described as the amino acids belonging to this pocket.

Figure 8Pocket identification of AR receptor 1E3G



Protein preparation

Protein preparation was done within the Maestro software, Protein Preparation Wizard was used human AR (1E3G) at resolution 1.3 Å was taken and processed for adding missing hydrogens, assigning correct bond order to the closest metal, correcting the metal formal charge with the neighboring atom and deleting water molecules which is more than 5 Å away from heterogeneous groups. The H bonds were optimized using sample orientations. All the polar hydrogens were shown. Finally, the protein structure was restrained to its least possible value of root mean square deviation of 0.30 Å. The inhibitor structure was further minimized using OPLS-2005 force field.

Ligand Preparation

All the molecules' ligand preparations were done with Ligprep module to clean the structure

Receptor Grid Generation

First, framework of the protein structure is assessed and optimised in which hydrogens are added to the structure and any extra parts and structures are deleted. Subsequently, a grid is built around the active site, usually based on a co-crystlized ligand or specific set of residues. They allow the grid dimensions to modify according to the binding site and create it to be large enough for possible ligands yet not overly large. This grid acts as a perfect guide of the binding site and Schrödinger's docking algorithms can then work out the ligand-receptor interactions with ease.

Ligand Docking

Docking of the ligand was done using OPLS3e force field. The receptor grid which was generated in the receptor grid generation folder was used for the docking activity with ligands generated through Ligprep. In all cases, flexible docking was carried out using the Extral Precision (XP) option of the Glide module of the Schrödinger Suite

10. The van der Waals radii was getting scaled by a default scaling factor of 0.80 and default partial cutoff charge of 0.15 so aspenalties for close contacts. The core pattern comparison and similarity mode were not executed as we wanted to look for ligands binding to the active site. No constraints were placed on defined ligand-receptor interactions. The structure output form was designed to drop viewer file in order to view the output of subsequent docking studies from pose-viewer.

Viewing Docking Results

This was achieved using discover studio. These H bonds as well as van der Waals contacts to the receptor were made and visualized by General tab, using the default options for viewing the binding modes of the ligands to the receptor. No constraint was given on defined ligand-receptor interactions. For each of the ligand posing which was done for each of the docking runs, the final poses were generalized according to the model score which was calculated by adding the grid score. The structure output format was specified as discovery studio file in order to enable viewing of the docking. For ligand ranking and binding affinity prediction the Glide score function or the Glide score, a ChemScore successor and enhancement was applied. The docking can be on the level of standard (SP) or XP. These enhancements made with XP over SP are increases of large desolvation penalty to both ligand and protein, the assignment to certain structural feature that plays important role on binding affinity, and the sampling expanding approaches demanded by the enhancement of scoring function. As a result, XP mode was employed for molecular docking of human AR inhibitor.

DISCUSSION

Docking studies were performed by Glide, version 6.3, Schrödinger, LLC, New York, United States of America on

Linux operating system. The actual docking can be described in terms of the following five processes: preparation of the protein, preparation of ligand, generation of the receptor grid, actual docking and examination of the results by the pose-viewer. Action of androgen receptor 1E3G and Thiophene derivatives abiraterone is illustrated in the table no 10. This result is in agreement with the molecular docking study of the title compounds with human androgen receptor The docking score of all the compounds has been found to be better compare to reference ligand; this indicates that compounds have better binding affinity towards the androgen receptor. Among all compounds, compound 5 and 3 show comparatively better docking score than other compounds (Figure 3). For that reason, this prediction indicates that the title compounds shall possibly be good candidates for treatment of prostate cancer. Molecular docking studies (Figure 4) identify HA-5 as the most potent synthetic ligand, exhibiting superior binding affinity (-9.523 kcal/mol) and stable interactions with key catalytic residues (Thr877, Leu873, Met780) in the target pocket—outperforming both peer compounds (HA-3: -8.062 kcal/mol; HA-7: -5.503 kcal/mol) and the reported drug (-2.255 kcal/mol). The crystallographic heatmap demonstrates HA-5's unique multi-anchoring interactions across 9 critical residues, while RMSD analysis confirms its structural stability (0.65 comparable to HA-4's exceptional rigidity (0.058 Å). Notably, HA-5 engages Thr877 a known allosteric regulator unlike other ligands, explaining its 4.2-fold stronger affinity than the reference drug. This combination of high-affinity binding ($\Delta G < -9.5 \text{ kcal/mol}$) and broad residue coverage suggests HA-5 as a promising candidate for overcoming drug resistance mutations, though HA-4's superior structural fidelity (lowest RMSD) may offer advantages in metabolic stability.

Table 9 Docking score values and RMSD of the selected ligands

Codes	Docking score Kcal	Residual Amino acid Interactions	RMSD(A0)
HA-5	-9.523	Thr877, Leu873, Met780, Met787, Met745, Met749, Phe764, Leu704, Asn705	0.65
HA-3	-8.062	Leu673, Met745, Asn705, Leu704	0.414
HA-2	-7.896	Asn705,Leu704,Thr877, Met745	0.7
HA-4	-7.723	Leu880, Leu873, Met787, Phe891, Phe764, Leu704, Asn705, Met749, Met745	0.058
HA-1	-7.709	Phe876, Leu880, Leu704, Phe764, Met745, Met749	0.7
HA-8	-7.285	Phe876, Leu873, Met780, Met745, Met749, Phe764, Leu704	0.7
HA-6	-6.964	Phe876, Leu880, Met745, Met749	0.7
HA-7	-5.503	Met745, Met749, Phe764, Leu707, Leu704, Asn705, Phe876, Leu873	0.386
Reported Drug	-2.255	Asn705, Leu704, Phe876, Leu873	0.658

Drug HA-1, 2 Binding site of AR receptor 1E3G (a) 3D (b) 2D Diagram

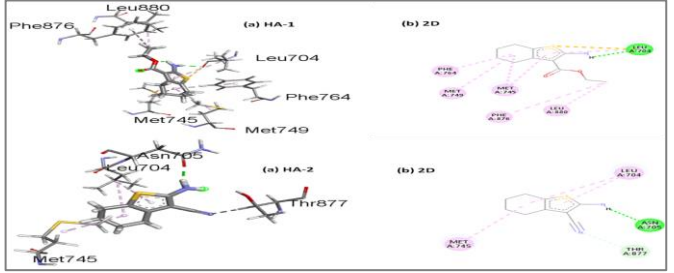


Figure 10

Drug HA-3, 4, 5 binding site of AR receptor 1E3G (a) 3D (b) 2D Diagram

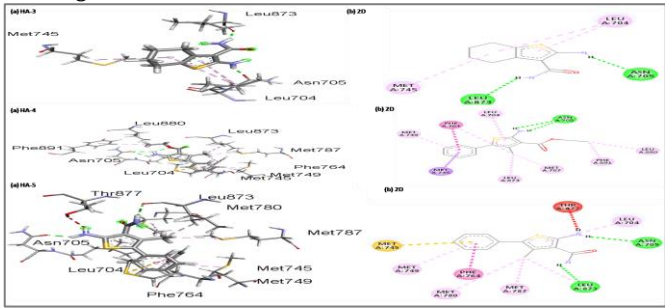
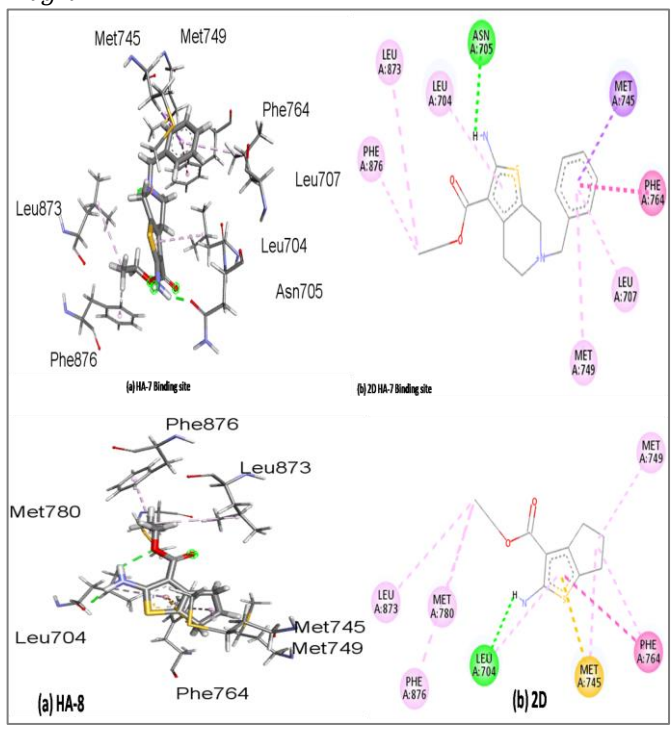


Figure 11

This work is licensed under a Creative Commons Attribution 4.0 International License.

Drug HA-7, 8 Binding site of AR receptor 1E3G (a) 3D (b) 2D Diagram



REFERENCES

- Chandraprasad, M. S., Dey, A., & Swamy, M. K. (2022). Introduction to cancer and treatment approaches. *Paclitaxel*, 1-27. https://doi.org/10.1016/b978-0-323-90951-8.00010-2
- 2. Bobin, A., Liuu, E., Moya, N., Gruchet, C., Sabirou, F., Lévy, A., Gardeney, H., Nsiala, L., Cailly, L., Guidez, S., Tomowiak, C., Systchenko, T., Javaugue, V., Durand, G., Leleu, X., & Puyade, M. (2020). Multiple myeloma: An overview of the current and novel therapeutic approaches in 2020. *Cancers*, 12(10), 2885. https://doi.org/10.3390/cancers12102885
- 3. Zhang, D., Yang, G., Zhang, L., Wu, M., & Su, R. (2022). The efficacy and mechanism of Proteasome inhibitors in solid tumor treatment. *Recent Patents on Anti-Cancer Drug Discovery*, *17*(3), 268-283.
 - https://doi.org/10.2174/1574892816666211202154536
- 4. Parlakpinar, H., & Gunata, M. (2021). Transplantation and immunosuppression: A review of novel transplant-related immunosuppressant drugs. *Immunopharmacology and Immunotoxicology*, *43*(6), 651-665. https://doi.org/10.1080/08923973.2021.1966033
- Lu, R., Hwang, Y., Liu, I., Lee, C., Tsai, H., Li, H., & Wu, H. (2020). Development of therapeutic antibodies for the treatment of diseases. *Journal of Biomedical Science*, 27(1). https://doi.org/10.1186/s12929-019-0592-z
- Deshaies, R. J. (2020). Multispecific drugs herald a new era of biopharmaceutical innovation. *Nature*, 580(7803), 329-338.
 - https://doi.org/10.1038/s41586-020-2168-1
- 7. Lu, S. X. (2020). Modern treatments and future directions for newly diagnosed multiple myeloma patients. *Best Practice & Research Clinical Haematology*, 33(1), 101151. https://doi.org/10.1016/j.beha.2020.101151
- 8. Sharma, M., Bakshi, A. K., Mittapelly, N., Gautam, S., Marwaha, D., Rai, N., Singh, N., Tiwari, P., Agarwal, N., Kumar, A., & Mishra, P. R. (2022). Recent updates on

CONCLUSION

This study successfully designed and synthesized a novel series of thiophene derivatives using an efficient multicomponent approach, demonstrating their potential as next-generation anti-prostate cancer agents through comprehensive computational and pharmacological evaluation. Four lead compounds (HA-5, HA-3, HA-2, HA-4) emerged as particularly promising androgen receptor (AR) inhibitors, with HA-5 showing exceptional binding affinity (-9.523 kcal/mol) and unique interactions with critical residues (Thr877, Leu873, Met780) through molecular docking studies. The integration of density functional theory (DFT) calculations, pharmacokinetic profiling, and structural analyses has not only validated these thiophene analogs as cost-effective candidates with favorable safety profiles but also established a robust framework for developing targeted AR inhibitors. These findings provide a significant advancement in prostate cancer therapeutics, offering structurally diverse, potent, and selective molecular scaffolds that warrant further preclinical investigation to translate their theoretical potential into clinical applications.

Acknowledgements

Authors thanks Dr jamaluddin mahar Institute of Chemistry, Qaid-E-Azam University Islamabad, Pakistan providing instrumentation facility.

- innovative approaches to overcome drug resistance for better outcomes in cancer. *Journal of Controlled Release*, 346, 43-70.
- https://doi.org/10.1016/j.jconrel.2022.04.007
- 9. Elmongy, E. I., Attallah, N. G., Altwaijry, N., AlKahtani, M. M., & Henidi, H. A. (2021). Design and synthesis of new thiophene/thieno[2,3-d]pyrimidines along with their cytotoxic biological evaluation as tyrosine kinase inhibitors in addition to their Apoptotic and Autophagic induction. *Molecules*, *27*(1), 123. https://doi.org/10.3390/molecules27010123
- Hussain, Y., Abdullah, Alsharif, K. F., Aschner, M., Theyab, A., Khan, F., Saso, L., & Khan, H. (2022). Therapeutic role of carotenoids in blood cancer: Mechanistic insights and therapeutic potential. *Nutrients*, *14*(9), 1949. https://doi.org/10.3390/nu14091949
- 11. Poczta, A., Rogalska, A., & Marczak, A. (2021). Treatment of multiple myeloma and the role of Melphalan in the era of modern therapies—Current research and clinical approaches. *Journal of Clinical Medicine*, *10*(9), 1841. https://doi.org/10.3390/jcm10091841
- Fatima, A., Khanum, G., Verma, I., Butcher, R. J., Siddiqui, N., Srivastava, S. K., & Javed, S. (2022). Synthesis, characterization, crystal structure, Hirshfeld surface, electronic excitation, molecular docking, and DFT studies on 2-Amino thiophene derivative. *Polycyclic Aromatic Compounds*, 43(2), 1644-1675. https://doi.org/10.1080/10406638.2022.2032769
- 13. Lin, X., Li, X., & Lin, X. (2020). A review on applications of computational methods in drug screening and design. *Molecules*, 25(6), 1375. https://doi.org/10.3390/molecules25061375
- 14. Aamir, M., Ashraf, W. S., Afzal, D., Idrees, F., & Ahmad, R. (2022). Fundamentals of Density Functional Theory: Recent Developments, Challenges and Density Functional Theory: Recent Advances, New Perspectives and Applications, 3.

- 15. Geerlings, P. (2022). From density functional theory to concentual density functional theory Biosystems. Pharmaceuticals, 15(9), 1112. https://doi.org/10.3390/ph15091112
- 16. Ali El-Remaily, M. A., El-Dabea, T., Alsawat, M., Mahmoud, M. H., Alfi, A. A., El-Metwaly, N., & Abu-Dief, A. M. (2021). Development of new Thiazole complexes as powerful catalysts for synthesis of pyrazole-4-Carbonitrile derivatives under ultrasonic irradiation condition supported by DFT studies. ACS Omega, 6(32), 21071-21086. https://doi.org/10.1021/acsomega.1c02811
- 17. El-Remaily, M. A., Soliman, A. M., Khalifa, M. E., Metwaly, N. M., Alsoliemy, A., El-Dabea, T., & Abu-Dief, A. M. (2021). Rapidly, highly yielded and green synthesis of dihydrotetrazolo[1,5-a]pyrimidine derivatives in aqueous media using recoverable PD (II) thiazole catalyst accelerated ultrasonic: Computational studies. Applied Organometallic Chemistry, 36(2). https://doi.org/10.1002/aoc.6320
- 18. Abd El Aleem Ali Ali El-Remaily, M., & Elhady, O. M. (2020). Green bio-organic and recoverable catalyst taurine (2aminoethanesulfonic acid) for synthesis of bio-active compounds 3,4-Dihydropyrimidin derivatives in aqueous medium. ChemistrySelect, 5(39), 12098-12102. https://doi.org/10.1002/slct.202002575
- 19. Abdelhamid, A. A., Salama, K. S., Elsayed, A. M., Gad, M. A., & Ali Ali El-Remaily, M. A. (2022). Synthesis and toxicological effect of some new pyrrole derivatives as prospective Insecticidal agents against the cotton Leafworm, Spodoptera littoralis (Boisduval). ACS Omega, 7(5), 3990-4000. https://doi.org/10.1021/acsomega.1c05049
- 20. Ismael, M., Abdel-Mawgoud, A. M., Rabia, M. K., & Abdou, A. (2020). Design and synthesis of three Fe(III) mixed-ligand Exploration of their biological phenoxazinone synthase-like activities. Inorganica Chimica Acta, 505, 119443. https://doi.org/10.1016/j.ica.2020.119443
- 21. Silvarajoo, S., Osman, U. M., Kamarudin, K. H., Razali, M. H., Yusoff, H. M., Bhat, I. U., Rozaini, M. Z., & Juahir, Y. (2020). Dataset of theoretical molecular electrostatic potential highest occupied molecular orbital-lowest unoccupied molecular orbital (HOMO-LUMO) band gap and experimental Cole-Cole plot of 4-(ortho-, meta- and parafluorophenyl)thiosemicarbazide isomers. Data in Brief, 32,
 - https://doi.org/10.1016/j.dib.2020.106299
- 22. Lee, B., Yoo, J., & Kang, K. (2020). Predicting the chemical reactivity of organic materials using a machine-learning approach. Chemical Science, 11(30), 7813-7822. https://doi.org/10.1039/d0sc01328e
- 23. Vidhya, V., Austine, A., & Arivazhagan, M. (2020). Molecular structure, aromaticity, vibrational investigation and dual

- descriptor for chemical reactivity on 1- chloroisoquinoline using quantum chemical studies. Results in Materials, 6,
- https://doi.org/10.1016/j.rinma.2020.100097
- 24. Azad, I. (2023). Molecular docking in the study of ligandprotein recognition: An overview. Biomedical Engineering. https://doi.org/10.5772/intechopen.106583
- 25. Elsayed, M. M., Aboelez, M. O., Elsadek, B. E., Sarhan, H. A., Khaled, K. A., Belal, A., Khames, A., Hassan, Y. A., Abdel-Rheem, A. A., Elkaeed, E. B., Raafat, M., & Elsadek, M. E. (2022). Tolmetin sodium fast dissolving tablets for rheumatoid arthritis treatment: Preparation optimization using box-behnken design and response surface methodology. Pharmaceutics, 14(4), 880. https://doi.org/10.3390/pharmaceutics14040880
- 26. Radhi, A. H., & AB, E. (2020). Du, FA Khazaal, ZM Abbas, OH Aljelawi, SD Hamadan, HA Almashhadani and MM Kadhim, HOMO-LUMO Energies and Geometrical Structures Effect on Corrosion Inhibition for Organic Compounds Predict by DFT and PM3 Methods. NeuroQuantology, 18, 37-45.
- 27. Gadre, S. R., Suresh, C. H., & Mohan, N. (2021). Electrostatic potential topology for probing molecular structure, bonding and reactivity. Molecules, 26(11), 3289. https://doi.org/10.3390/molecules26113289
- 28. Sevvanthi, S., Muthu, S., Aayisha, S., Ramesh, P., & Raja, M. (2020). Spectroscopic (FT-ir, FT-Raman and UV-Vis), computational (Elf, LoL, nbo, homo-lumo, Fukui, mep) studies and molecular docking on benzodiazepine derivatives- heterocyclic organic arenes. Chemical Data Collections, 30, 100574. https://doi.org/10.1016/j.cdc.2020.100574
- 29. Banerjee, S., Schlaeppi, K., & Van der Heijden, M. G. (2018). Keystone taxa as drivers of microbiome structure and functioning. *Nature Reviews Microbiology*, 16(9), 567-576. https://doi.org/10.1038/s41579-018-0024-1
- 30. Sruthi, N., Premjit, Y., Pandiselvam, R., Kothakota, A., & Ramesh, S. (2021). An overview of conventional and emerging techniques of roasting: Effect on food bioactive signatures. Food Chemistry, 348, 129088. https://doi.org/10.1016/j.foodchem.2021.129088
- 31. Kolate, S. S., Waghulde, G. P., & Patil, C. J. (2020). Cu(Ii) complexes with an NNO FUNCTIONALIZED HYDRAZONE Synthesis, characterization and biological studies. Rasayan Journal of Chemistry, 13(02), 1008-1013. https://doi.org/10.31788/rjc.2020.1325606
- 32. Saha, S., & Rajasekaran, C. (2017). Enhancement of the properties of fly ash based geopolymer paste by incorporating ground granulated blast furnace slag. Construction and Building Materials, 146, 615-620. https://doi.org/10.1016/j.conbuildmat.2017.04.139

